

Higgs-like Excitations of Cold Atom System with Spin-orbit Coupling

Fei-Jie Huang[†], Qi-Hui Chen[†], Wu-Ming Liu^{†*}

¹*National Laboratory for Condensed Matter Physics, Institute of Physics, Chinese Academy of Sciences, Beijing 100190, China*

[†]*These authors contributed equally to this work.*

^{*}*e-mail: wliu@iphy.ac.cn*

The Higgs-like excitations, which distinguish from the Higgs amplitude mode in many-body system, are single-particle excitations in system with non-Abelian gauge potential. We investigate the Higgs-like excitations of cold atom system in artificial non-Abelian gauge potential. We demonstrate that when a non-Abelian gauge potential is reduced to Abelian potential, its Abelian part constructs spin-orbit coupling, and its non-Abelian part emerges Higgs-like excitations. The Higgs-like excitations induce a mass of the non-Abelian gauge field, which offsets the defect of massless of the gauge theories. We show that the mass of gauge field can affect the spin Hall currents which are produced by the spin-orbit coupling. We also discuss the observation of these phenomena in real experiment.

The Higgs type excitations are significant for both particle physics and condensed matter physics. In particle physics, the Higgs type excitations generate the mass of particle. In condensed matter physics, the Higgs type excitations relate to order phase of the system. In particle physics,

the suspected Higgs boson has been found by the Large Hadron Collider (LHC) in 2012 ^{1,2}. In condensed matter physics, the Higgs amplitude mode, which is massive amplitude mode of collective excitations in many-body system, appears from superconductors ³ to superfluids ⁴⁻⁸. However, all these results were concerned with the Higgs amplitude mode in many-body systems, an investigation of the Higgs-like excitations is still absent. The Higgs-like excitations are single-particle excitations in system with non-Abelian gauge potential, the emergence of Higgs-like excitations is due to the breaking of parallel transportation of non-Abelian gauge potential, which connects to the spin-orbit (SO) coupling of the system.

The SO coupling, which is the interaction between the spin and the momentum of a particle, is related to many effects in condensed matter physics ⁹⁻¹². Recently, with the realization of various artificial gauge potentials, the cold atom system also can be designed to simulate SO coupling ¹³⁻¹⁶. This opens a new arena to explore novel effects in cold atoms ¹⁷⁻²⁸. The key of simulating SO coupling is the synthesis of non-Abelian gauge potentials by engineering the interaction between the atoms and the lasers ¹⁶. It is well known that the non-Abelian gauge potentials play a crucial role in understanding the fundamental interactions in particle physics. In condensed matter physics, the non-Abelian gauge potentials also appear in study of the mechanism of high- T_c superconductivity ³ and graphene ²⁹.

In this report, we will investigate the Higgs-like excitations of cold atom system in non-Abelian gauge potential. We first synthesize a $SU(2)$ gauge potential in cold atom system. By reducing the $SU(2)$ gauge potential to $U(1)$ potential, we analyze the Abelian and non-Abelian

parts of the gauge potential. We find that the Abelian part of the gauge potential constructs SO coupling, and its non-Abelian part emerges Higgs-like excitations. We show that the Higgs-like excitations give rise to a mass of the gauge field, while the mass can affect the spin Hall currents induced by SO coupling. Finally, we discuss how to observe these phenomena through the detection of spin Hall currents in real experiment.

Results

The spin-orbit coupling of cold atom system. We consider a cold atom system with each atom having a three-level Λ -type configuration as shown in Fig. 1. Two ground states $|g_1\rangle$ and $|g_2\rangle$ are coupled to an excited state $|e\rangle$ through the laser fields. The Rabi frequencies are taken as $\Omega_1 = \frac{1}{2}\Omega[\exp(i\mathbf{k} \cdot \mathbf{r}) + \exp(i\mathbf{k}' \cdot \mathbf{r})]$ and $\Omega_2 = \frac{1}{2i}\Omega[\exp(i\mathbf{k} \cdot \mathbf{r}) - \exp(i\mathbf{k}' \cdot \mathbf{r})]$, in which \mathbf{k} and \mathbf{k}' are the wave vectors of lasers, $\mathbf{k}' = e^{i\varphi}\mathbf{k}$, \mathbf{r} is the position vector, φ is an angle between the lasers as shown in Fig. 1b. The total Rabi frequency is given by $\Omega = (|\Omega_1|^2 + |\Omega_2|^2)^{1/2}$. The Hamiltonian of cold atom reads $H = H_k + H_I + V_{trap}$, in which $H_k = p^2/2m$ is the kinetic energy, p is the momentum, m is the atomic mass, V_{trap} is a trapping potential. The interacting Hamiltonian is given by $H_I = 2\Delta |e\rangle\langle e| + (\Omega_1 |e\rangle\langle g_1| + \Omega_2 |e\rangle\langle g_2| + h.c.)$, where Δ is the detuning.

For large detuning, by utilizing Berry phase, the eigenstates of the interacting Hamiltonian will give rise to an effective $SU(2)$ gauge potential (See Method section) $\mathbf{A} = \frac{1}{2}\mathbf{q}\sigma_y + \frac{1}{4}\delta^2\mathbf{Q}\sigma_z$, where $\sigma_i, i = x, y, z$ are the Pauli matrices, $\mathbf{Q} = \mathbf{k} + \mathbf{k}'$ is the total wave vector of the laser fields and $\mathbf{q} = \mathbf{k} - \mathbf{k}'$ is the relative wave vector, $\delta = \arctan[(\frac{\Delta^2}{\Omega^2} + 1)^{1/2} - \frac{\Delta}{\Omega}]$. Redefining

this effective potential to a $SU(2)$ scalar gauge potential $\mathcal{A}_0 = [\gamma, \mathbf{A}]_+$, where $[\cdot]_+$ is an anti-commutator, $\gamma = \mathbf{p}/p$ is a dimensionless parameter. Then neglecting the trapping potential and the constant terms, the effective Hamiltonian of cold atom reads

$$H = H_k + g\mathcal{A}_0 + V, \quad (1)$$

in which $H_k = \eta p$ is the kinetic energy, $g = \eta$ is an effective charge, $\eta = p/2m$ is a non-relativistic dimensionless strength factor (assuming the light velocity $c = 1$), $V = \frac{1}{16m}\delta^2[q^2 - (1 + \delta^2)Q^2]\sigma_z + \delta\frac{\Omega}{2}\sigma_z = M_0\sigma_z$ is a scalar potential originating from construction of \mathbf{A} .

It is generally known that the SO coupling appears in $U(1)$ gauge potential, hence to construct SO coupling, let's reduce the $SU(2)$ gauge potential \mathcal{A}_0 to $U(1)$ potential. Firstly, we denote $\mathbf{n} = (n_x, n_y, n_z)$ as a unit vector which follows the direction of magnetic field, and define the direction vector of internal $SU(2)$ space as $\sigma(t) = n_i\sigma_i(t)$, where t is time, $i = x, y, z$. The definition implies that we have chosen the same directions for the external and the internal spaces at the initial time. Then along the direction vector σ , \mathcal{A}_0 will be decomposed to two gauge potentials $\mathcal{A}_0 = \mathcal{A} + \mathcal{B}$ ^{30,31}, with

$$\begin{aligned} \mathcal{A} &= (\sigma \cdot \mathcal{A}_0)\sigma + [\partial_0\sigma, \sigma], \\ \mathcal{B} &= [\sigma, \nabla_0\sigma], \end{aligned} \quad (2)$$

where $\nabla_0 = \partial_0 + [\mathcal{A}_0, \cdot]$ represents the time component of covariant derivative, $[\cdot, \cdot]$ denotes the commutator. According to reduction theorem, when \mathcal{A}_0 is reducible to $U(1)$ potential, there should be

$$\nabla_0\sigma = 0. \quad (3)$$

Therefore, if \mathcal{A}_0 is a $U(1)$ potential, $\mathcal{A}_0 = \mathcal{A}$. We view \mathcal{A} is the Abelian part of \mathcal{A}_0 , and the potential \mathcal{B} is the non-Abelian part.

Now let's discuss the physical meaning of the constraint condition $\nabla_0 \sigma = 0$. This condition actually is a parallel transportation. Taking the Planck constant $\hbar = 1$, $\partial_0 = i\partial_t$ will correspond to Hamiltonian operator. Neglecting the scalar potential V and setting the effective charge $g = 1$, we obtain $[\sigma, H] = [\sigma, \mathcal{A}_0]$, the constraint condition becomes

$$i\partial_t \sigma = [\sigma, H]. \quad (4)$$

This equation is nothing but the equation of motion of spin. Therefore, the constraint condition in fact corresponds to the equation of motion of spin, and the direction vector σ corresponds to the spin operators of the system, as shown in Fig. 2.

We conclude that, only when the non-Abelian gauge potential \mathcal{A}_0 satisfies the constraint condition $\nabla_0 \sigma = 0$, \mathcal{A}_0 is suited for constructing SO coupling. If the constraint condition can not be satisfied, the gauge potential \mathcal{B} in \mathcal{A}_0 will exist and only \mathcal{A} is suited for constructing SO coupling in this case.

We now add the scalar potential V to the effective Hamiltonian to check whether \mathcal{A}_0 satisfies the constraint condition or not. The constraint condition can be rewritten as $\nabla_0 \sigma = [\sigma, H] + [\mathcal{A}_0, \sigma]$. Because the scalar potential is a non-Abelian potential, we find $\nabla_0 \sigma \neq 0$. In this situation, the SO coupling term of cold atom reads $H_{SO} = g\mathcal{A}$, with its explicit expression

$$H_{SO} = \lambda \sigma_y + \nu \sigma_z. \quad (5)$$

The coupling strength factors λ and ν are $\lambda = \frac{1}{m}[\frac{1}{2}\mathbf{q} \cdot \mathbf{p} + \delta^3 \Omega p(\mathbf{Q} \cdot \mathbf{p} / \mathbf{q} \cdot \mathbf{p})]$ and $\nu = \frac{1}{m}(-2\delta \Omega p + 2^{-2} \delta^2 \mathbf{Q} \cdot \mathbf{p}) + \frac{1}{4m^2} \delta^2 (Q^2 - q^2)p$, respectively, in which the initial direction of σ is pointed to \mathcal{A}_0 in the $SU(2)$ space.

Higgs-like excitations of cold atom system. Since the non-Abelian gauge potential \mathcal{A}_0 does not satisfy the constraint condition, there will be a residual term left in the Hamiltonian after constructing SO coupling. This term can be expressed as $H_{k,B} = g\mathcal{B}$, with $\mathcal{B} = -\frac{\mathbf{Q} \cdot \mathbf{p}}{\mathbf{q} \cdot \mathbf{p}} \delta^3 \Omega \sigma_y + [2\delta \Omega + \frac{1}{4m} \delta^2 (Q^2 - q^2)] \sigma_z$. The potential \mathcal{B} is a gauge covariant potential, it has a mass term $M_B^2 \text{Tr}[\mathcal{B} \cdot \mathcal{B}]$. Writing down the action of non-Abelian gauge field, the mass reads $M_B = M_0 / (1 + (\mathbf{Q} \cdot \mathbf{p} / 2\mathbf{q} \cdot \mathbf{p})^2 \delta^4)^{\frac{1}{2}}$ (See Method section). Consequently, the effective Hamiltonian of cold atom can be written as $H = H_k + H_{SO} + H_B$, in which

$$H_B = H_{k,B} + \eta' M_B \sigma_z. \quad (6)$$

It is clear that the Hamiltonian H_B describes an excitation. $H_{k,B} = g\mathcal{B}$ can be viewed as the kinetic energy of the coupling between the excitation and the atom. The scalar potential $V = \eta' M_B \sigma_z$ in fact describes the coupling between the mass of the excitation and the atom, where $\eta' = (1 + (\mathbf{Q} \cdot \mathbf{p} / 2\mathbf{q} \cdot \mathbf{p})^2 \delta^4)^{\frac{1}{2}}$ is a dimensionless coupling factor.

Let's discuss the origin of the excitation. As shown in Fig. 2, the original direction of σ presents $SU(2)$ symmetry in the internal space, its direction can be chosen freely. Nevertheless, when \mathcal{A}_0 is used to construct SO coupling, the direction of σ is confined to the constraint condition, and the initial symmetry is broken. Yet in general, the whole \mathcal{A}_0 can not be suited for constructing SO coupling, so there is a trend to restore the initial symmetry. The potential \mathcal{B} just plays the

role of an excited field which restores the initial symmetry. We treat the excitation as Higgs-like excitation. Due to the excitation, the gauge field \mathcal{A}_0 obtains mass. Note that the excitations are different from the appearance of Higgs bosons in dynamic gauge field. The appearance of Higgs bosons requires local gauge invariance, while the gauge field discussed here is induced by Berry phase, it is not dynamic and lack the local gauge invariance.

The impact of Higgs-like excitations to spin Hall currents. The trajectories of single cold atom contributed by excitation can be calculated from the equation of motion $\dot{\mathbf{r}} = -i[\mathbf{r}, H_B]$. As shown in Fig. 3a, the contribution includes two opposite trajectories. The Fig. 3b shows the dispersion of H_B . The dispersion is linear, and the energy does not vanish at zero momentum due to the presence of excited mass M_B .

Next, let's discuss the impact of the excitations to the cold atom system. A two-dimensional harmonic potential $\frac{1}{2}m\omega^2(y^2 + z^2)$ is chosen to trap the cold atoms. The relationship between the particle number N and the trap frequency ω can be obtained by solving the equation

$$N = \int d\mathbf{r} n(r, t = 0, T = 0), \quad (7)$$

in which

$$n(r, t, T) = \frac{1}{(2\pi)^2} \int d\mathbf{p} [f_+(p, r, t, T) + f_-(p, r, t, T)] \quad (8)$$

is the density profile of the cold atom system, $f_{\sigma_z} = f_{\pm}(p, r, t, T) = [e^{\beta(H_{\pm}(p, r, t) - \mu)} + 1]^{-1}$ are the spin-dependent Fermi distributions with $\beta = 1/k_B T$, k_B and T are the Boltzmann constant and

temperature. The Hamiltonian is given by (See Method section)

$$H_{\pm}(p, r, t) = \frac{p^2}{2m} \pm \left(\frac{\mathbf{q} \cdot \mathbf{p}}{2m} + M_B \right) + \frac{1}{2}m\omega^2 z^2 + \frac{1}{2}m\omega^2 \left(1 \pm \frac{2m^*}{M_B} \right) \left(y \pm \frac{\mathbf{q} \cdot \mathbf{p}}{2m} t \right)^2. \quad (9)$$

where $m^* = q^2/2m$ is a characteristic mass of the system. The relationship is shown in Fig. 4.

We now discuss the spin Hall currents of the system. In order to generate spin Hall currents, the wave vectors of the lasers are chosen as $k_x = k'_x = 0$, the internal space is rotated $\pi/2$ around the x direction. In this case, the SO coupling reads $H_{SO} = \lambda\sigma_z$. This term describes the spin Hall currents in which the spin is polarized to z direction while the currents move along y direction. The spin Hall currents can be written as

$$J_{\sigma_z}^y = \frac{1}{(2\pi)^2} \int d\mathbf{p} f_{\sigma_z}(p) j_{\sigma_z}^y, \quad (10)$$

where $j_{\sigma_z}^y = \langle \hat{j}_{\sigma_z}^y \rangle$ are the single particle currents, $\hat{j}_{\sigma_z}^y = \frac{1}{4}[\sigma_z, v_y]_+$ are the spin current operators, $v_y = -i[y, H]$ is the velocity along y direction. The impact of the excitations to the spin Hall currents is shown in Fig. 5a. It demonstrates that the spin down current is suppressed by the increase of the excited mass, while the spin up current grows slightly. The evolution of the atomic density profile $n(r, t)$ is shown in Fig. 5b.

Experimental signatures of Higgs-like excitations. Let's discuss the observation of the Higgs-like excitations by detecting the spin Hall currents. We can choose ${}^6\text{Li}$ atoms for a three-level Λ -type system, the particle number is about 10^4 , a $2\pi \times 10^2 \text{ Hz}$ harmonic potential is used to trap the atoms. The configuration of four laser fields is shown in Fig. 1b. The wave number of the lasers can be taken as $2\pi \times 1.0(\mu\text{m})^{-1}$ ¹⁵. For a large detuning, the Rabi frequency and the detuning are

required to satisfy $\Omega^2/\Delta \sim 10^6 Hz$. When the laser fields are turned on, a non-Abelian gauge potential is applied to the 6Li atoms. By tuning the angle φ between the lasers, different masses of excitations can be obtained.

To detect the spin up current, we firstly initialize the atoms in $|g_1\rangle$ state. Then a Raman pulse is applied between the states $|g_1\rangle$ and $|g_2\rangle$ to transfer the atoms to spin up state $|\chi_{D1}\rangle$. The Rabi frequency of the pulse is required to match the spatial variation of $|\chi_{D1}\rangle$. Turning on the lasers, the cold atoms will experience the SO coupling, and couple to the excitations. After a time t , we turn off the lasers and apply a reversal Raman pulse to transfer the atoms back to the initial state. By using the time of flight measurement, the spin up current of the system can be determined. The measurement of the spin down current (corresponding to the $|\chi_{D2}\rangle$ state) also can be detected in the same manner^{32,33}.

Discussion

In this report, we investigated the Higgs-like excitations, which distinguish from the Higgs amplitude mode, in cold atom system. In condensed matter physics, the Higgs amplitude mode is collective excitations which are generated by interactions between particles in many-body system, the interactions induce the system to go through a spontaneous breaking of continuous symmetry, and the Higgs amplitude mode emerges. Nevertheless, the Higgs-like excitations are single-particle excitations which have nothing to do with interactions between particles, as shown by Fig. 2, the emergence of Higgs-like excitations is due to the breaking of parallel transportation of non-Abelian

gauge potential. Moreover, the Higgs amplitude mode is independent of the SO coupling, while the Higgs-like excitations can connect to SO coupling.

The impact of the Higgs-like excitations to the spin Hall currents is shown in Fig. 5. It demonstrates that the spin down current is suppressed, while the spin up current grows slightly by the increase of the excited mass. We discuss how to observe the Higgs-like excitations through the detection of spin Hall currents in real experiment.

It should be noted that the results we obtain not only confine in cold atom system, but also can apply to systems concerning Berry phase. We expect that the exploration of Higgs-like excitations of cold atom system can help to understand the mass generation mechanism both in the condensed matter physics and in particle physics.

Methods

$SU(2)$ gauge potential \mathcal{A}_0 . The Hamiltonian of cold atom reads $H = H_k + H_I + V_{trap}$, in which $H_k = p^2/2m$ is the kinetic energy, p is the momentum, m is the atomic mass, V_{trap} is a trapping potential. The interacting Hamiltonian is given by $H_I = 2\Delta |e\rangle\langle e| + (\Omega_1 |e\rangle\langle g_1| + \Omega_2 |e\rangle\langle g_2| + h.c.)$, where Δ is the detuning.

Defining $\mathbf{Q} = \mathbf{k} + \mathbf{k}'$ as the total wave vector of the laser fields, $\mathbf{q} = \mathbf{k} - \mathbf{k}'$ as the relative wave vector, $\delta = \arctan[(\frac{\Delta^2}{\Omega^2} + 1)^{1/2} - \frac{\Delta}{\Omega}]$, $\phi = \frac{1}{2}\mathbf{Q} \cdot \mathbf{r}$, $\theta = \frac{1}{2}\mathbf{q} \cdot \mathbf{r}$, then the eigenvectors of

interacting Hamiltonian can be expressed as

$$\begin{aligned}
|\chi_{D1}\rangle &= -\sin\theta|g_1\rangle + \cos\theta|g_2\rangle, \\
|\chi_{D2}\rangle &= -\exp(i\phi)\sin\delta|e\rangle + \cos\delta\cos\theta|g_1\rangle + \cos\delta\sin\theta|g_2\rangle, \\
|\chi_3\rangle &= \exp(i\phi)\cos\delta|e\rangle + \sin\delta\cos\theta|g_1\rangle + \sin\delta\sin\theta|g_2\rangle,
\end{aligned} \tag{11}$$

with the eigenvalues are $0, \frac{\Omega}{2\Delta}, 2\Delta$, respectively.

For large detuning, we can neglect the eigenvalue 2Δ and assume the other two eigenvalues are degeneracy, hence by utilizing Berry phase, the remaining two eigenvectors of the interacting Hamiltonian will give rise to an effective $SU(2)$ gauge potential $\mathbf{A}_{\alpha\beta} = -i\langle\chi_\alpha|\nabla|\chi_\beta\rangle$, $\alpha, \beta = D1, D2$, with its explicit expression

$$\mathbf{A} = \frac{1}{2}\mathbf{q}\sigma_y + \frac{1}{4}\delta^2\mathbf{Q}\sigma_z, \tag{12}$$

where $\sigma_i, i = x, y, z$ are the Pauli matrices. Redefining potential \mathbf{A} , we obtain $SU(2)$ gauge potential

$$\mathcal{A}_0 = [\gamma, \mathbf{A}]_+, \tag{13}$$

where $[\cdot, \cdot]_+$ is an anti-commutator, $\gamma = \mathbf{p}/p$ is a dimensionless parameter.

The mass of the gauge field. Because the gauge field has only time component \mathcal{A}_0 , we can expand the action of the gauge field as

$$S = Tr F_{0i}F_{0i} + \frac{1}{2}Tr F_{00}F_{00}, \tag{14}$$

where 0 is the time component index and i are space component indices, respectively. It is obvious that the second term of the expansion is the mass term. When \mathcal{A}_0 is substituted to the mass term,

we have

$$\frac{1}{2}Tr F_{00}F_{00} = M_B^2 Tr[\mathcal{B} \cdot \mathcal{B}], \quad (15)$$

in which the mass reads

$$M_B = M_0 / (1 + (\mathbf{Q} \cdot \mathbf{p} / 2\mathbf{q} \cdot \mathbf{p})^2 \delta^4)^{\frac{1}{2}}. \quad (16)$$

Derivation of the Hamiltonian (9). The wave vectors of the lasers are chosen as $k_x = k'_x = 0$, the internal space is rotated $\pi/2$ around the x direction. Combining the Eq. (5) and Eq. (6), the explicit expression of Hamiltonian can be written as

$$H(p, r) = \frac{p^2}{2m} + \frac{\mathbf{Q} \cdot \mathbf{p}}{4m} \delta^2 \sigma_y + \frac{\mathbf{q} \cdot \mathbf{p}}{2m} \sigma_z + \eta' M_B \sigma_z + \frac{1}{2} m \omega^2 (y^2 + z^2). \quad (17)$$

Diagonalizing the Hamiltonian and expanding in M_B order, we have

$$H_{\pm}(p, r) = \frac{p^2}{2m} \pm \left(\frac{\mathbf{q} \cdot \mathbf{p}}{2m} + M_B \right) + \frac{1}{2} m \omega^2 z^2 + \frac{1}{2} m \omega^2 \left(1 \pm \frac{2m^*}{M_B} \right) y^2, \quad (18)$$

in which $m^* = q^2/2m$ is a characteristic mass of the system. From $\dot{\mathbf{r}} = -i[\mathbf{r}, H]$, the time evolved Hamiltonian can be obtained

$$H_{\pm}(p, r, t) = \frac{p^2}{2m} \pm \left(\frac{\mathbf{q} \cdot \mathbf{p}}{2m} + M_B \right) + \frac{1}{2} m \omega^2 z^2 + \frac{1}{2} m \omega^2 \left(1 \pm \frac{2m^*}{M_B} \right) \left(y \pm \frac{\mathbf{q} \cdot \mathbf{p}}{2m} t \right)^2. \quad (9)$$

1. Incandela, J. CMS talk at *Latest update in the search for the Higgs boson* at CERN, July4, 2012, <https://cms-docdb.cern.ch/cgi-bin/PublicDocDB//ShowDocument?docid=6125>.
2. Gianotti, F. ATLAS talk at *Latest update in the search for the Higgs boson* at CERN, July4, 2012, <https://cms-docdb.cern.ch/cgi-bin/PublicDocDB//ShowDocument?docid=6126>.

3. Lee, P. A., Nagaosa, N., Wen, X. G. Doping a Mott insulator: Physics of high-temperature superconductivity. *Rev. Mod. Phys.* **78**, 17 (2006).
4. Volovik, G. E. *Exotic properties of superfluid ^3He* , (World Scientific, 1992).
5. Huber, S. D., Theiler, B., Altman, E. & Blatter, G. Amplitude mode in the quantum phase model. *Phys. Rev. Lett.* **100**, 050404 (2008).
6. Cooper, F., Chien, C. C., Mihaila, B., Dawson, J. F. & Timmermans, E. Composite-field Goldstone states and Higgs mechanism in dilute Bose gases. *Phys. Rev. A* **85**, 023631 (2012).
7. Pollet, L. & Prokof'ev, N. Higgs mode in a two-dimensional superfluid. *Phys. Rev. Lett.* **109**, 010401 (2012).
8. Endres, M., *et al.* The Higgs amplitude mode at the two-dimensional superfluid-Mott insulator transition. *Nature* **487**, 454 (2012).
9. Murakami, S., Nagaosa, N. & Zhang, S. C. Dissipationless quantum spin current at room temperature. *Science* **301**, 1348 (2003).
10. Sinova, J., Culcer, D., Niu, Q., Sinitsyn, N. A., Jungwirth, T. & MacDonald, A. H. Universal intrinsic spin Hall effect. *Phys. Rev. Lett.* **92**, 126603 (2004).
11. Hasan, M. Z. & Kane, C. L. Colloquium: topological insulators. *Rev. Mod. Phys.* **82**, 3045 (2010).
12. Qi, X. L. & Zhang, S. C. Topological insulators and superconductors. *Rev. Mod. Phys.* **83**, 1057 (2011).

13. Lin, Y. J., Jiménez-García, K., Porto, J. V., & Spielman, I. B. Spin-orbit-coupled Bose-Einstein condensates. *Nature* **471**, 83 (2011).
14. Wang, P., *et al.* Spin-orbit coupled degenerate Fermi gases. *Phys. Rev. Lett.* **109**, 095301 (2012).
15. Cheuk, L. W., *et al.* Spin-injection spectroscopy of a spin-orbit coupled Fermi gas. *Phys. Rev. Lett.* **109**, 095302 (2012).
16. Dalibard, J., Gerbier, F., Juzeliūnas, G. & Öhberg, P. Colloquium: Artificial gauge potentials for neutral atoms. *Rev. Mod. Phys.* **83**, 1523 (2011).
17. Ruseckas, J., Juzeliūnas, G., Öhberg, P. & Fleischhauer, M. Non-abelian gauge potentials for ultracold atoms with degenerate dark states. *Phys. Rev. Lett.* **95**, 010404 (2005).
18. Zhu, S. L., Fu, H., Wu, C. J., Zhang, S. C. & Duan, L. M. Spin Hall effects for cold atoms in a light-induced gauge potential. *Phys. Rev. Lett.* **97**, 240401 (2006).
19. Liu, X. J., Borunda, M. F., Liu, X. & Sinova, J. Effect of induced spin-orbit coupling for atoms via laser fields. *Phys. Rev. Lett.* **102**, 046402 (2009).
20. Wang, C., Gao, C., Jian, C. M. & Zhai, H. Spin-orbit coupled spinor Bose-Einstein condensates. *Phys. Rev. Lett.* **105**, 160403 (2010).
21. Iskin, M. & Subasi, A. L. Stability of spin-orbit coupled Fermi gases with population imbalance. *Phys. Rev. Lett.* **107**, 050402 (2011).

22. van der Bijl, E. & Duine, R. A. Anomalous Hall conductivity from the dipole mode of spin-orbit-coupled cold-atom systems. *Phys. Rev. Lett.* **107**, 195302 (2011).
23. Sinha, S., Nath, R. & Santos, L. Trapped two-dimensional condensates with synthetic spin-orbit coupling. *Phys. Rev. Lett.* **107**, 270401 (2011).
24. Hu, H., Jiang, L., Liu, X. J. & Pu, H. Probing anisotropic superfluidity in atomic Fermi gases with Rashba spin-orbit coupling. *Phys. Rev. Lett.* **107**, 195304 (2011).
25. Liao, R., Yi-Xiang, Y. & Liu, W. M. Tuning the tricritical point with spin-orbit coupling in polarized Fermionic condensates. *Phys. Rev. Lett.* **108**, 080406 (2012).
26. Deng, Y., Cheng, J., Jing, H., Sun, C. P. & Yi, S. Spin-orbit-coupled dipolar Bose-Einstein condensates. *Phys. Rev. Lett.* **108**, 125301 (2012).
27. Ozawa, T. & Baym, G. Stability of ultracold atomic Bose condensates with Rashba spin-orbit coupling against quantum and thermal fluctuations. *Phys. Rev. Lett.* **109**, 025301 (2012).
28. Zhang, J. Y. *et al.* Collective dipole oscillations of a spin-orbit coupled Bose-Einstein condensate. *Phys. Rev. Lett.* **109**, 115301 (2012).
29. Vozmediano, M. A. H., Katsnelson, M. I., Guinea, F. Gauge fields in graphene. *Phys. Rep.* **496**, 109 (2010).
30. Faddeev, L. & Niemi, A. J. Partially Dual Variables in SU(2) Yang-Mills Theory. *Phys. Rev. Lett.* **82**, 1624 (1999).

31. Faddeev, L. & Niemi, A. J. Spin-charge separation, conformal covariance and the SU(2) Yang-Mills theory. *Nucl. Phys. B* **776**, 38 (2006).
32. Stanescu, T. D., Zhang, C. & Galitski, V. Nonequilibrium spin dynamics in a trapped fermi gas with effective spin-orbit interactions. *Phys. Rev. Lett.* **99**, 110403 (2007).
33. Olson, A. J., Niffenegger, R. J. & Chen, Y. P. Optimizing the efficiency of evaporative cooling in optical dipole traps. *Phys. Rev. A* **87**, 053613 (2013).

Acknowledgement This work was supported by NKBRSCF under grants Nos. 2011CB921502, 2012CB821305, the NSFC under grants Nos. 61227902.

Author Contributions All authors planned and designed theoretical numerical studies. All contributed in completing the paper.

Competing Interests The authors declare that they have no competing financial interests.

Correspondence Correspondence and requests for materials should be addressed to Liu, Wu-Ming.

Figure 1 The configuration of three-level Λ -type atoms interacting with laser fields. (a) Two ground states $|g_1\rangle$ and $|g_2\rangle$ are coupled to an excited state $|e\rangle$ through the laser fields. Ω_1 and Ω_2 are the Rabi frequencies, Δ is a large detuning. (b) Two inner laser fields (the blue arrows) are arranged to form Rabi frequency Ω_1 , other two lasers (the red arrows) are arranged to form Ω_2 . There is an angle φ between the laser fields.

Figure 2 The sphere surface of $SU(2)$ gauge potential \mathcal{A}_0 . (a) At the initial time $t = 0$, the basic vectors of the gauge potential $\sigma_x(0)$, $\sigma_y(0)$ and $\sigma_z(0)$ point to certain directions. The direction vector (the red arrow) $\sigma(0)$ points to A . (b) After a time t , the basic vectors change to $\sigma_x(t)$, $\sigma_y(t)$ and $\sigma_z(t)$ directions. The direction vector $\sigma(t)$ changes along with the basic vectors and points to B . If the path AB satisfies the equation of motion of spin, the SO coupling will present. If not, then excepting for SO coupling, Higgs-like excitation will emerge.

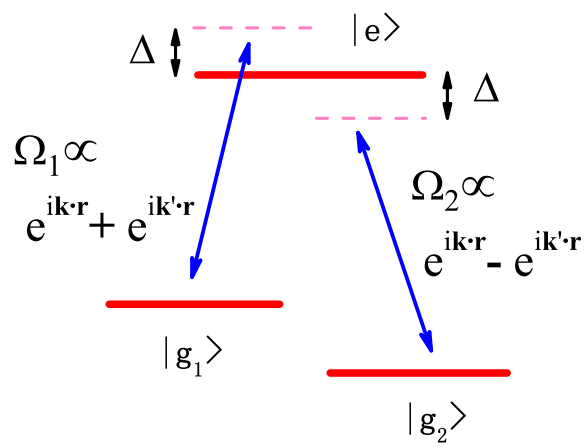
Figure 3 The impact of Higgs-like excitation to single cold atom. (a) The trajectories of a single cold atom contributed by Higgs-like excitation. The red solid line and the blue dash line correspond to the velocities $v = 3 \times 10^{-3} \mu m/s$ and $v = 5 \times 10^{-3} \mu m/s$, respectively. (b) The dispersion of coupling energy between the Higgs-like excitation and a single atom, $\varepsilon_B = (\epsilon p + \eta' M_B) \sigma_z$. The red solid line and the blue dash line correspond to the coupling strength parameters $\epsilon = 4m^{-1} \times 10^{-2}$ and $\epsilon = 6m^{-1} \times 10^{-2}$, respectively. The unit of the energy ε_B is the recoil energy $\varepsilon_R = k^2/(2m)$.

Figure 4 The relationship between the particle number N and the trap frequency ω . ε_F

is the Fermi energy. The red solid line and the blue dash line correspond to the ratios $M_B/m^* = 2.2$ and $M_B/m^* = 2.8$, respectively.

Figure 5 The impact of Higgs-like excitations to spin Hall currents. (a) The relationship between the excited mass M_B and the spin Hall currents $J_{\sigma_z}^y$, in which the spin is polarized to z direction while the currents move along y direction. The red (blue) line corresponds to the spin up (down) current. The unit of $J_{\sigma_z}^y$ is $\frac{1}{2\pi} \times 10cm/s$. (b) The evolution of the atomic density profile from the time $t = 0ms$ to $t = 4ms$ and $t = 9ms$. The red and blue parts in each figure denote the spin up and spin down atoms. The unit of y and z directions is μm . The temperature is taken as $T = 0.4T_F$, T_F is the Fermi temperature. The up and down figures correspond to the ratios $M_B/m^* = 2.2$ and $M_B/m^* = 2.8$, respectively. The figures show the trends of spin currents of Fig. 5a.

(a)



(b)

